RESEARCH PAPER

Channels 5:6, 489-499; November/December 2011; © 2011 Landes Bioscience

Residual Cx45 and its relationship to Cx43 in Murine ventricular myocardium

Mingwei Bao,[1,†] Evelyn M. Kanter,[1] Richard Y.C. Huang,[2] Stephan Maxeiner,[5,‡] Marina Frank,[5] Yan Zhang,[1] Richard B. Schuessler,[3] Timothy W. Smith,[1] R. Reid Townsend,[1,4] Henry W. Rohrs,[2] Viviana M. Berthoud,[6] Klaus Willecke,[5] James G. Laing[1] and Kathryn A. Yamada[1,*]

[1]Department of Medicine; [2]Department of Chemistry; [3]Department of Surgery; [4]Department of Cell Biology and Physiology; Washington University School of Medicine; St. Louis, MO USA; [5]Institute of Genetics; University of Bonn; Bonn, Germany; [6]Department of Pediatrics; University of Chicago; Chicago, IL USA

[†]Current Affiliation: Department of Cardiology; Renmin Hospital of Wuhan University; Wuhan, Hubei China; [‡]Neurosciences Institute; Stanford School of Medicine; Palo Alto, CA USA

Key words: connexin45, gap junctions, quantitative immunoblots, co-immunoprecipitation, electron microscopy, Cx45 phosphorylation, CaMKII, transgenic mice

Abbreviations: Cx, connexin; Cx45, connexin45; Cx43, connexin43; Cx30.2, connexin30.2; Cx31.9, connexin31.9; Cx40, connexin40; GST, glutathione S-transferase; CaMKII, Ca^{2+}/calmodulin-dependent protein kinase II; CK1, casein kinase 1; WT, wild-type; Cx45OEs, mice with cardiac-selective overexpression of Cx45; LV, left ventricular; RV, right ventricular; AV, atrio-ventricular; SA, sino-atrial; PCR, polymerase chain reaction; α-MHC, alpha-myosin heavy chain; fl, floxed; $Cx40^{KICx45/KICx45}$, Cx40 knockin Cx45 mice; CT, carboxy-terminal; MS, mass spectrometry; SDS, sodium dodecyl sulfate; IB, immunoblotting

Gap junction channels in ventricular myocardium are required for electrical and metabolic coupling between cardiac myocytes and for normal cardiac pump function. Although much is known about expression patterns and remodeling of cardiac connexin (Cx)43, little is known about the less abundant Cx45, which is required for embryonic development and viability, is downregulated in adult hearts, and is pathophysiologically upregulated in human end-stage heart failure. We applied quantitative immunoblotting and immunoprecipitation to native myocardial extracts, immunogold electron microscopy to cardiac tissue and membrane sections, electrophysiological recordings to whole hearts, and high-resolution tandem mass spectrometry to Cx45 fusion protein, and developed two new tools, anti-Cx45 antisera and Cre^{+};Cx45 floxed mice, to facilitate characterization of Cx45 in adult mammalian hearts.

We found that Cx45 represents 0.3% of total Cx protein (predominantly 200 fmol Cx43 protein/μg ventricular protein) and colocalizes with Cx43 in native ventricular gap junctions, particularly in the apex and septum. Cre^{+};Cx45 floxed mice express 85% less Cx45, but do not exhibit overt electrophysiologic abnormalities. Although the basal phosphorylation status of native Cx45 remains unknown, CaMKII phosphorylates eight Ser/Thr residues in Cx45 in vitro.

Thus, although downregulation of Cx45 does not produce notable deficits in electrical conduction in adult, disease-free hearts, Cx45 is a target of the multifunctional kinase CaMKII, and the phosphorylation status of Cx45 and the role of Cx43/Cx45 heteromeric gap junction channels in both normal and diseased hearts merits further investigation.

Introduction

Cardiac myocyte gap junctions are large specialized aggregates of intercellular channels responsible for cell-to-cell communication. Their role is essential for propagation of electrical activity that is required for cardiac function. Cardiac gap junction channels are formed by connexins, each of which imparts distinct biophysical properties depending on the connexin subtype.[1-4] Three of the five connexins expressed in cardiac myocytes are found in ventricular myocardium. Of those three, Cx43 is the predominant connexin expressed in working ventricular myocytes and is responsible for electrical propagation throughout the chamber walls.[5] The other two, Cx45 and Cx30.2, are expressed primarily in the cardiac conduction system;[6,7] however, the human ortholog, Cx31.9, is not expressed in the human cardiac conduction system.[8] Cx40 is expressed in the atria.[9-11] Most recently, Gros et al.[12] have shown that Cx30 is expressed in the mouse sino-atrial (SA) node. Of note, Cx45 is absolutely required for cardiac development; genetic ablation of Cx45 is embryonic lethal.[13,14] It is the only connexin protein whose absence during embryonic development is incompatible with life. Nevertheless, it appears that Cx45 may not be at all necessary for normal cardiac function post-natally.

As stated above, Cx45 is localized at the endocardial surface of ventricular myocardium[15] in a distribution overlapping that of

*Correspondence to: Kathryn A. Yamada; Email: kyamada@wustl.edu
Submitted: 07/19/11; Revised: 10/24/11; Accepted: 10/25/11
http://dx.doi.org/10.4161/chan.5.6.18523

Cx40-expressing myocytes of the conduction system. Expression of Cx45 by adult working ventricular myocytes is limited.[13,16] We have demonstrated that Cx45 is distributed throughout working ventricular myocardium of both adult murine and adult human hearts.[17,18] Indeed, Cx45 is responsible for cell-to-cell coupling in Cx43-null myocytes.[19] Because the expression level of Cx45 relative to Cx43 is so much smaller, the contribution of Cx45 to intercellular current flow is thought to be minimal. However, we have shown that Cx45 is upregulated in human failing hearts,[18] and that increased expression of Cx45 enhances susceptibility to ventricular tachyarrhythmias in vivo.[20] Thus, Cx45 may influence electrical and/or metabolic coupling as a result of pathophysiological remodeling of gap junctions such as that observed after heart failure or myocardial infarction.

Cardiac connexins have been shown to interact and form heteromeric channels in vitro in heterologous expression systems.[21-29] Several studies have reported the consistent finding that expression of Cx45 (~29 pS channels) in cells expressing Cx43 (~90 pS channels) results in a dominant negative effect characterized by reduced gap junctional conductance and dye transfer.[23-25] These observations suggest that the absolute abundance of different connexin proteins in gap junction channels and the relative stoichiometry of multiple connexins within each channel in ventricular myocytes are two important determinants of whole cell junctional conductances.

To date, Cx43/Cx45 heteromeric gap junction channels have not been identified definitively nor studied systematically in native ventricular myocytes. Although there is currently no direct evidence that Cx45/Cx43 heteromeric channels function in native hearts, the wide spectrum of single channel conductances observed in pairs of isolated cardiac myocytes,[30-33] coupled with the multitude of studies demonstrating heteromeric channel function in in vitro expression systems[21-29,34-36] implicate the presence of Cx43/Cx45 heteromeric channels in the heart. The purpose of the present study was to determine the absolute level of Cx45 protein relative to Cx43 in native ventricular myocardium from the adult mouse, and to establish whether Cx45 plays a role in cardiac conduction properties in non-failing hearts. We have obtained biochemical and ultra-structural evidence for coexistence of Cx43 and Cx45 in gap junctions of working ventricular myocytes. In addition, although the level of Cx45 protein expression was reduced by ~85% in cardiac-restricted Cx45-deficient mice, no defects in cardiac conduction parameters were observed. Post-translational modification of Cx45, a potential regulatory mechanism for the expression and stability of Cx45, was also explored.

Results

Specificity of the monoclonal antibodies used for the quantitative immunoblots is shown in **Figure 1 and Figure S3**. Each antibody detected its respective CT fusion protein and connexin protein in ventricular samples, but not the other fusion protein or connexin in ventricular samples. The anti-Cx43 antibody detected either GST-Cx43 CT fusion protein (**Fig. 1**) or thrombin-cleaved Cx43 CT alone (**Fig. S3**).

Absolute expression levels of Cx45 and Cx43 in native mouse ventricular myocardium. Quantitative immunoblots were performed by loading different amounts of six His-Cx45 CT and GST-Cx43 CT fusion proteins along with samples of ventricular homogenates (**Fig. 1**). The band densities of the ventricular homogenates fell within the linear portion of the standard curves for the fusion proteins. As expected, Cx43 protein levels far exceeded those of Cx45. Mean data from 16 hearts (**Table 1**) show that ventricular myocardium contained 215 ± 103 fmol of Cx43/μg protein. Our average protein yield from a larger group of 24 hearts was 127 ± 16 μg protein/mg wet weight of ventricular tissue, and the ventricles weighed 112 ± 15 mg wet weight (n = 24). Thus, based on these averages, we observed 27 pmol Cx43 protein per mg wet weight of tissue, and the ventricles of each heart expressed 3 nmol of Cx43. Cx45 protein expression in murine ventricular myocardium, on the other hand, was 0.7 ± 0.2 fmol/μg protein, or 10 pmol of Cx45 per heart, or 0.3% of total ventricular connexin protein levels (**Table 1**).

Relative expression of Cx45 and Cx43 in ventricular gap junctions. Despite the relatively low abundance of Cx45 in ventricular myocardium, double label immunoelectron microscopy of vibratome sections of murine ventricular myocardium demonstrated that Cx45- as well as Cx43-bound colloidal gold particles were found together in the same gap junction plaques (data not shown). All subsequent analyses were performed on gap junction-enriched membrane preparations (**Fig. 2A**). The majority (87%) of gap junctions isolated from WT hearts was labeled only with Cx43 (**Fig. 2A, left** and **B**). Double label immunoelectron microscopy of gap junction-enriched membrane fractions using a pre-embedding staining protocol showed more abundant labeling of Cx43 (96%) than Cx45 (4%) in plaques isolated from the 13% of WT gap junctions that contained both Cx43 and Cx45 (**Fig. 2A, right** and **C**). The combined Cx43 signal (87% plus 0.96 of 13%, or 12.5% in heteromeric junctions) of 99.5% is consistent with the quantitative immunoblot data (99.7%).

Previously, we reported that Cx45OEs exhibit a 2-fold increase in Cx45 immunoreactive signal and a 25% increase in total Cx45 protein on immunoblots.[20] In the present study, we analyzed gap junction-enriched preparations isolated from WT and Cx45OE hearts. We found a larger percentage of heteromeric junctions (55% compared to 13% in wild-type hearts) in preparations isolated from Cx45OE hearts (**Fig. 2B**). However, the relative stoichiometry of Cx43:Cx45 was comparable in the 55% of Cx45OE gap junctions that contained both connexins; the relative abundance of Cx43 and Cx45 in gap junctional plaques containing both Cx43 and Cx45 was ~95:5 in both WT and Cx45OE hearts (**Fig. 2C**). Of note, no gap junctions containing Cx45 alone were found in either genotype. Not surprisingly, there was more Cx45 staining as a percentage of total Cx43 plus Cx45 found in preparations isolated from Cx45OE (4.1%) compared to WT hearts (1.4%). Finally, the percentage of heteromeric gap junctions containing both Cx43 and Cx45 was higher in gap junction-enriched membrane preparations isolated from the LV apex plus septum compared to those isolated from the LV free wall, consistent with more Cx45 expressed in the ventricular conduction system (**Fig. 2D**).

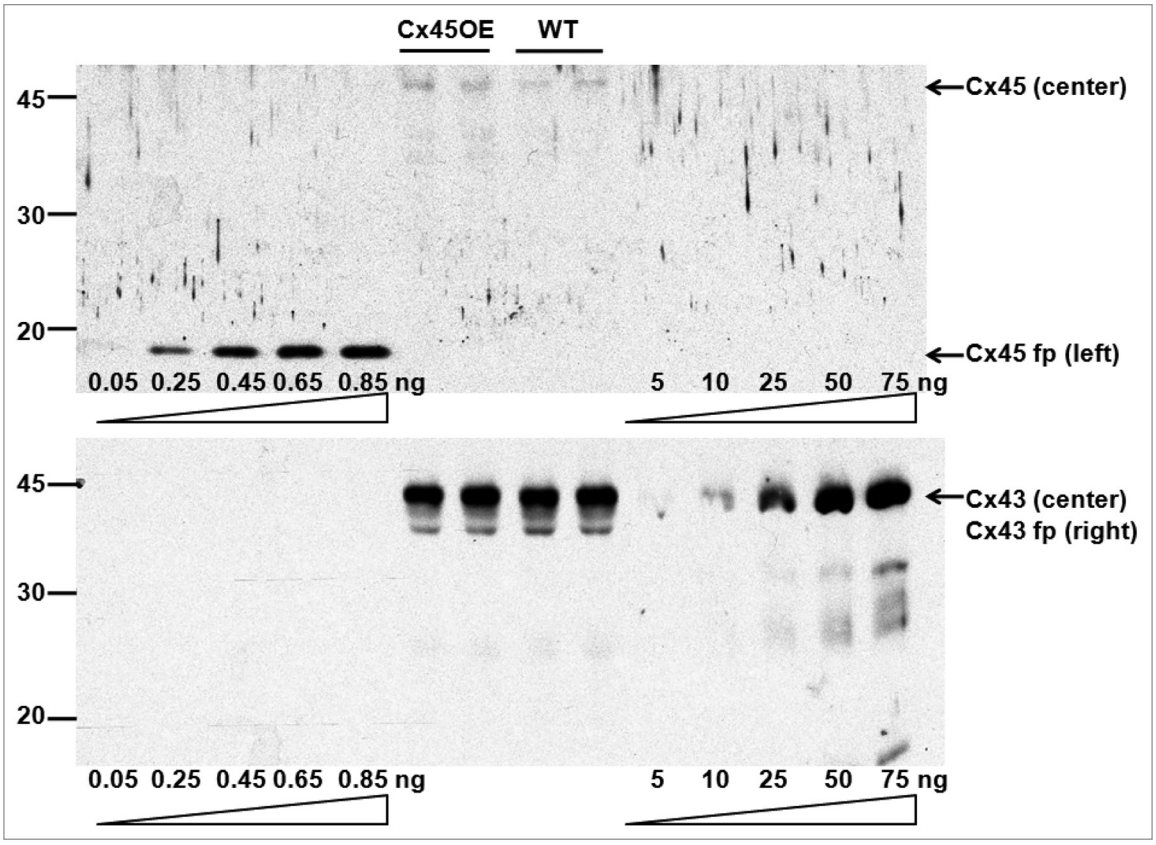

Figure 1. Representative quantitative immunoblots of a membrane probed first with anti-Cx45 antiserum (top), stripped, then reprobed with anti-Cx43 antibody (bottom). The gel was loaded with increasing amounts of Cx45 fusion protein (fp, five lanes on the left), ventricular homogenates from Cx45OE and wild-type (WT) mice (15 μg protein, four lanes in the middle), and increasing amounts of GST-Cx43 fusion protein (fp, five lanes on the right). The anti-Cx45 antiserum recognized only the Cx45 fusion protein at ~16 kD (top gel, left lanes) and Cx45 in the ventricular homogenates (top gel, center lanes), but not the Cx43 fusion protein (top gel, right lanes). The anti-Cx43 antibody, on the other hand, recognized only the GST-Cx43 fusion protein at ~43 kD (bottom gel, right lanes) and Cx43 in the ventricular homogenates (bottom gel, center lanes), but not the Cx45 fusion protein (bottom gel, left lanes).

Co-precipitation of Cx43 and Cx45 from ventricular myocardium. Ventricular lysates prepared from WT mice were subjected to immunoprecipitation. Immunoblotting with anti-Cx45 antibody demonstrated that Cx45 was co-precipitated with proteins immunoprecipitated with anti-Cx43 antibody (**Fig. 3**). In addition, Cx43 was co-precipitated with proteins immunoprecipitated with anti-Cx45 antibody (**Fig. 3**).

Neither cardiac-restricted reduction nor overexpression of Cx45 significantly alters electrophysiological properties of the heart in vitro. Despite the overall low abundance of Cx45 in adult working ventricular myocytes, it is critical for development of the heart and vasculature.[13,14] Mice with germline ablation of Cx45 die at embryonic day 10.5. Cx45 is present in the SA node and conduction system,[7,15,46] where it can largely replace Cx40, producing normal propagation in the atrio-ventricular (AV) node and left bundle branch and partial loss of function in the right bundle branch as shown in transgenic mice in which Cx45 was engineered to replace Cx40.[39] The question of whether Cx45 plays any role in conduction has been difficult to assess in the absence of survival of mice with germline ablation of Cx45, and in the absence of suitable antibodies directed against Cx45.

Table 1. Concentration of Cx43 and Cx45 in ventricular myocardium

	Per μg protein loaded on gel	Per mg wet weight of tissue	Per heart (ventricles)
Cx43 (n = 12)	215 ± 103 fmol/μg protein	27 pmol/mg wet weight	3 nmol
Cx45 (n = 16)	0.7 ± 0.2 fmol/μg protein	0.09 pmol/mg wet weight	10 pmol

Per tissue and per heart values were calculated using the following average empirical values obtained from 24 hearts: 127 μg protein/mg wet weight of ventricular tissue and 112 mg wet weight of RV + LV.

In the present study, we created a line of mice with Cx45-deficient hearts (**Fig. 4**) in both our Bonn and St. Louis laboratories. Mice were not born with the expected Mendelian inheritance pattern, suggesting either transient embryonic activation of the α-MHC promoter or a survival advantage of perinatal expression of Cx45 protein. Only 9 Cre^{+};$Cx45^{fl/fl}$ mice were born out of 87 pups in 17 litters (**Table 2**). One mouse died before weaning; one mouse died after weaning but before it could be

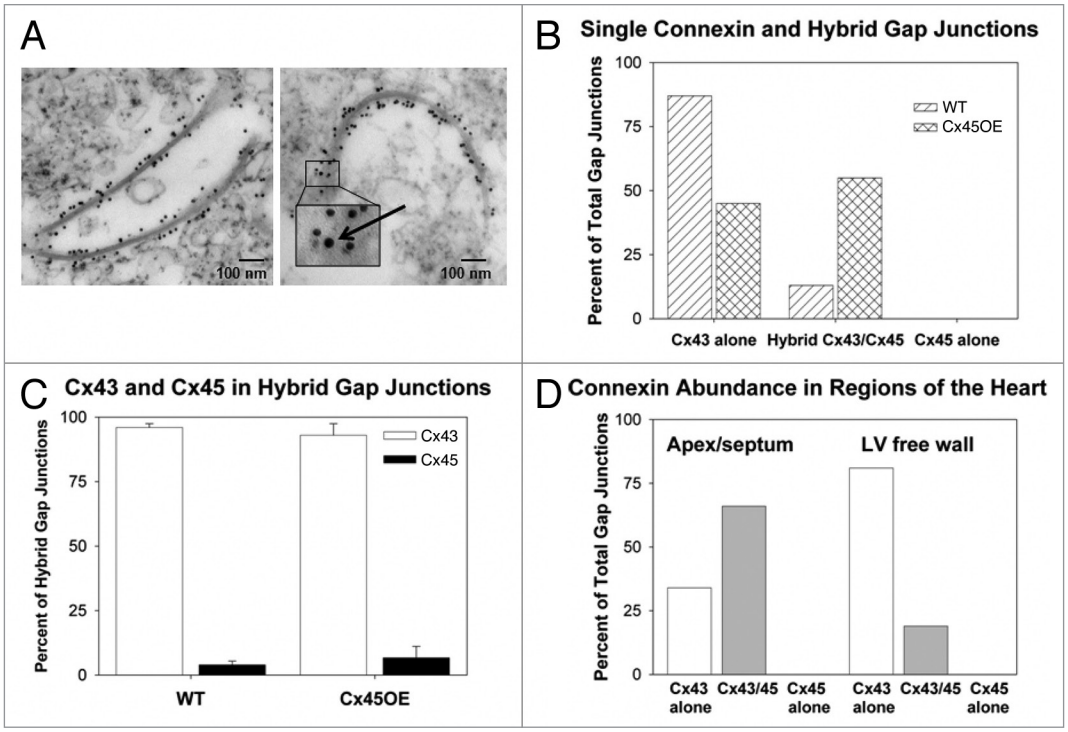

Figure 2. Immunogold electron microscopy of cardiac connexins in hybrid (heteromeric and/or heterotypic) gap junctions. (A) Electron micrographic images of gap junctions decorated with 10 nm gold particles conjugated with anti-Cx43 antiserum (left), and a gap junction containing a 20 nm gold particle conjugated to anti-Cx45 antiserum (inset, arrow) among numerous 10 nm gold particles conjugated to anti-Cx43 antibody (right). Bar = 100 nm. (B) Proportions of Cx43-bound gold particles and Cx45-bound gold particles as a percent of total gap junctions in gap junction-enriched membrane preparations isolated from wild-type (WT) and Cx45OE hearts. WT hearts exhibited a larger percentage (87%) of homomeric/homotypic Cx43 gap junctions. In contrast, the percentages of Cx43 only and heteromeric gap junctions in Cx45OE hearts were roughly equivalent. Cx45 homomeric/homotypic gap junctions were not found in either WT or Cx45OE hearts. (C) The percentage of Cx43 and Cx45 in heteromeric gap junction channels was comparable in WT and Cx45OE hearts, despite the fact that there was a greater proportion of heteromeric gap junction channels in Cx45OE hearts. (D) Relative proportions of Cx43 homomeric/homotypic and Cx43/Cx45 heteromeric gap junctions by gross regions of the hearts. More heteromeric gap junctions were observed in the apex/septum compared to the LV free wall consistent with known expression of Cx45 in the cardiac conduction system which is concentrated in the subendocardial interventricular septum and in the distal Purkinje system.

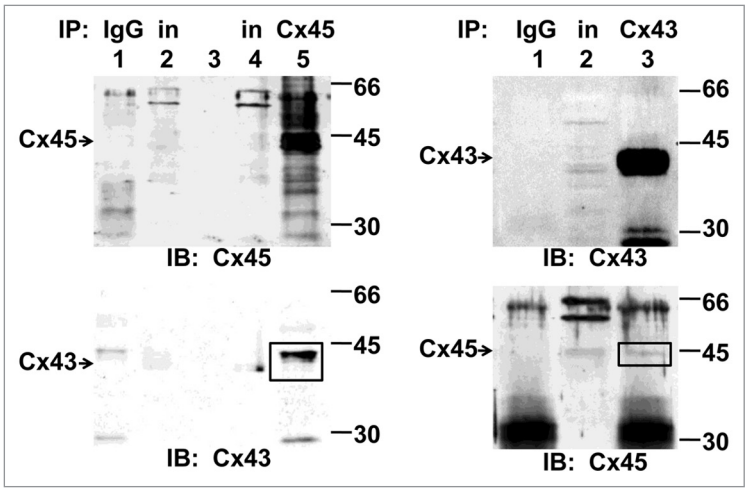

Figure 3. Co-immunoprecipitation of Cx43 and Cx45 from murine ventricular myocardium. Cx45 (upper left, lane 5) or Cx43 (upper right, lane 3) were immunoprecipitated (IP) using mouse monoclonal anti-Cx45 or anti-Cx43 antibodies bound to protein G sepharose beads, respectively. The proteins in the immunoprecipitates were resolved by SDS-polyacrylamide gel electrophoresis and subjected to immunoblotting (IB) with rabbit polyclonal anti-Cx43 and anti-Cx45 antibodies to reveal Cx43 (square) in Cx45-associated proteins (lower left, lane 5) and Cx45 (square) in Cx43-associated proteins (lower right, lane 3). Neither Cx43 nor Cx45 were observed in the negative controls in which mouse IgG1 was bound to protein G sepharose beads (IgG). In, supernatant of ventricular homogenates (input).

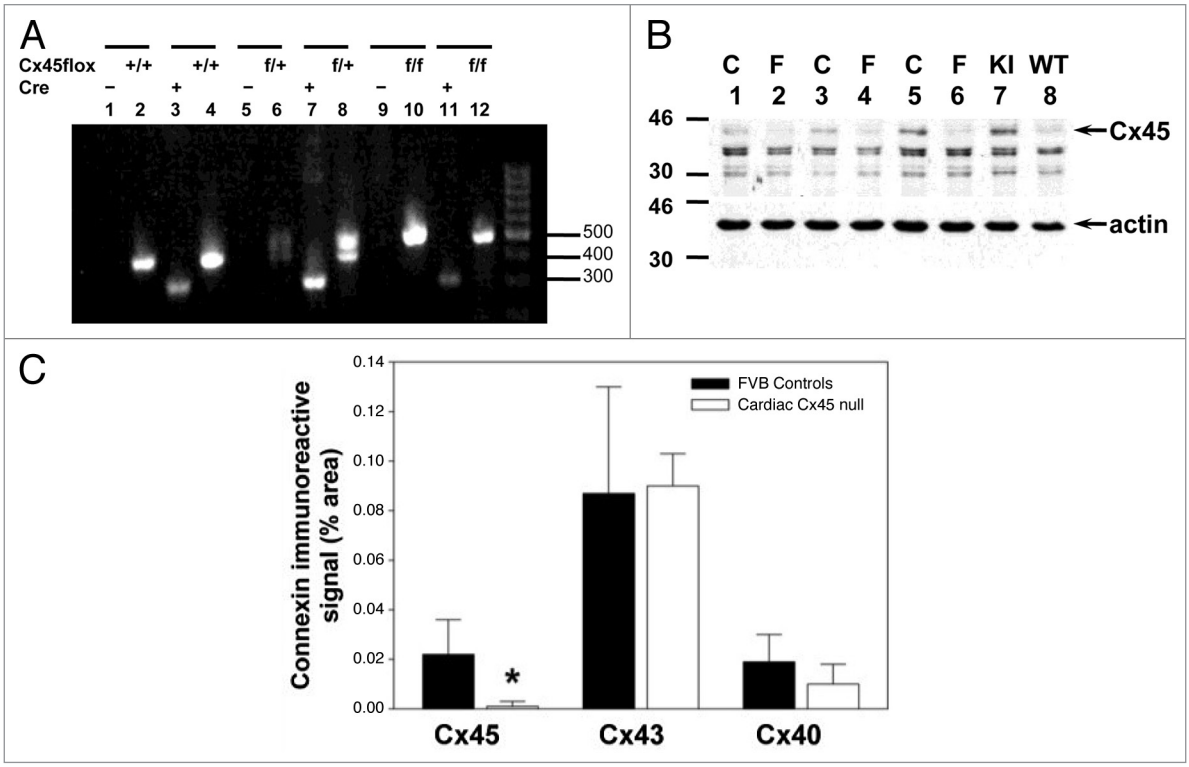

Figure 4. Cardiac-restricted ablation of Cx45 was accomplished by crossing Cx45 floxed mice with α-MHC-Cre$^+$ mice. (A) Agarose gel showing banding patterns of the PCR products used to genotype cardiac-restricted ablation of Cx45. DNA samples from 6 different mice were run on this gel. Two PCR reactions were run for each mouse to determine whether they carried the Cre transgene (lanes 1, 3, 5, 7, 9 and 11) and whether they carried two wild-type, a wild-type and a floxed, or two floxed alleles (lanes 2, 4, 6, 8, 10 and 12). The sizes of the bands are as follows: Cx45 wild-type allele, 380 kb; Cx45 floxed allele, 500 kb; Cre transgene, 292 kb. (B) Immunoblot of cardiac Cx45-deficient (Cre$^+$;Cx45$^{fl/fl}$) whole ventricular homogenates (F; lanes 2, 4 and 6) and controls (C; lanes 1, 3 and 5) showing markedly reduced Cx45 in Cre$^+$;Cx45$^{fl/fl}$ ventricles. Lane 7 shows a strong Cx45 band in atrial homogenate from Cx40KO/Cx45 knockin (KI) compared to the weaker Cx45 band in wild-type atrial homogenate (WT) shown in lane 8. The membrane was stripped and reprobed with anti-actin antibodies to show equal protein (20 μg) loading. (C) Histograms show summarized data of the confocal analysis of ventricular tissue sections stained with anti-Cx45, anti-Cx43 and anti-Cx40 antibodies. Values represent connexin immunoreactive signal as a percent of total tissue area (mean ± SD). Cx45 was significantly reduced in cardiac Cx45-deficient hearts. *p = 0.016.

studied. Of the seven remaining Cx45 cardiac-deficient mice, four mice were studied electrophysiologically. Immunoblotting (n = 6 Cx45-deficient mice) and immunostaining (n = 5 Cx45-deficient mice) were performed using a new anti-Cx45 antiserum whose characterization is described in the **Supplemental Material and Methods**. As expected, Cx45 protein expression was reduced in Cx45-deficient hearts (**Fig. 4B**). Residual levels of Cx45 were still present in whole ventricular homogenates prepared from Cre$^+$;Cx45$^{fl/fl}$ mice. Immunofluorescence images demonstrated an 85% reduction in Cx45 immunoreactive signal in Cx45-deficient hearts compared to controls (**Fig. 5**, left parts). Using ImageJ, we quantified Cx45, Cx43 and Cx40 immunoreactive signal in ventricular myocardium and found that only Cx45 was reduced in Cx45-deficient hearts (**Fig. 4C**). Cx40 signal was analyzed in the conduction system located in the subendocardial region of the interventricular septum and was unchanged in cardiac Cx45-deficient compared to control hearts (**Fig. 4C**).

Although cardiac Cx45-deficient mice were not born in the expected numbers, those that were born did not have any gross functional defects and survived to adulthood. Two Cre$^+$;Cx45$^{fl/fl}$ mice gave birth to offspring that themselves grew to adulthood. Their surface ECGs appeared normal (data not shown). QRS complexes were comparable to those recorded from control mice (**Fig. S4**); QRS duration in cardiac Cx45-deficient mice was 11.2 ± 1.2 ms (n = 4, p = 0.367) compared to 10.5 ± 1.1 ms in FVB controls (n = 5). Mean ventricular effective refractory periods were 110 ms for cardiac Cx45-deficient hearts (n = 2) compared with 123 ± 19 ms for controls (n = 3). We measured activation times between the RV apex and the LV lateral free wall to assess conduction through the specialized conduction system compared with that through the ventricular myocardium. Conduction during sinus rhythm is expected to result in nearly simultaneous activation of the right and left ventricles; this was indeed observed as shown in **Table S1**; activation of right and left ventricles occurred within 1 ms of each other, both in FVB controls (0.7 ± 1.2 ms) and in cardiac Cx45-deficient hearts (0.3 ms). Pacing from the right atrium produced similar activation times as those observed during sinus rhythm (0.6 ± 0.7 ms in controls vs. 1.0 ms in cardiac Cx45-deficient hearts). Pacing from the RV apex produced the expected activation delay through the ventricular myocardium (12.5 ± 2.7 ms); a comparable mean delay (15.4 ms) was observed in the two cardiac Cx45-deficient hearts.

Table 2. Cardiac Cx45-deficient mice

No. of litters	Mating	No. of pups born	Expected nulls (% of pups born)	Actual nulls (% of pups born)
10	$Cre^{-};Cx45^{fl/fl}$ x $Cre^{+};Cx45^{fl/+}$	52	13 (25%)	3 (6%)
6	$Cre^{-};Cx45^{fl/fl}$ x $Cre^{+};Cx45^{fl/fl}$	30	15 (50%)	5 (17%)
1	$Cre^{+};Cx45^{fl/fl}$ x $Cre^{+};Cx45^{fl/+}$	5	2.5 (50%)	1 (20%)
Total **17**		**87**	**30.5 (35%)**	**9 (10%)**

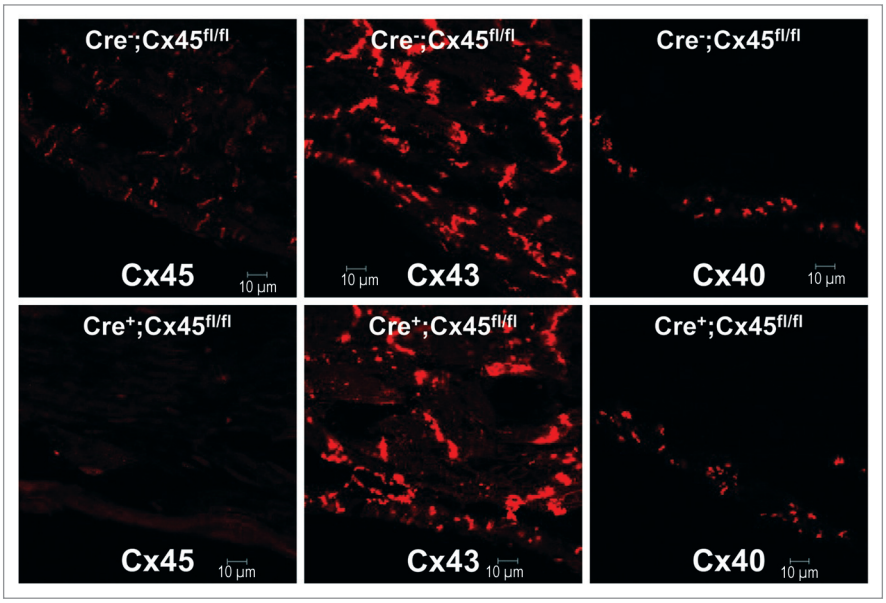

Figure 5. Representative confocal images from a control heart (upper three parts) and a $Cre^{+};Cx45^{fl/fl}$ heart (lower three parts) showing lack of Cx45 staining in the ventricle of the cardiac-restricted Cx45-deficient heart (lower left part). Adjacent tissue sections were stained for Cx45, Cx43 and Cx40, and every effort was made to select the same region in each heart for comparison. The ventricular chamber is at the bottom of each field. The subendocardial conduction system can be seen most clearly in the images stained for Cx40 (right parts). Cx43 and Cx45 are each expressed in this same region as well as in the ventricular myocardium beyond the subendocardial layer in the control heart (upper middle and left parts, respectively). Cx43 immunostaining is comparable in the control and $Cre^{+};Cx45^{fl/fl}$ hearts (upper and lower middle parts, respectively). Bars = 10 μm.

Although the number of mice studied was too low to perform statistical analyses, these data suggest that ablation of cardiac Cx45 does not adversely affect cardiac conduction. Isochronal maps demonstrating conduction in two cardiac Cx45-deficient hearts also indicate no difference in conduction velocity or patterns compared to those in control hearts; one example is shown in **Figure S5**.

Previously, we found that Cx45OEs exhibited increased susceptibility to inducible ventricular arrhythmias compared to WT littermate controls.[20] In the present study, we performed in vitro electrophysiology studies on perfused hearts. We calculated conduction velocities from optical action potentials elicited after S1 stimulation at the RV apex (180 ms cycle length) and after S2 stimulation at the center of the LV lateral free wall (140 ms coupling interval) in five Cx45OEs and six WT littermates. We found no significant differences in conduction velocities or anisotropic ratios recorded from Cx45OE versus WT hearts (**Table S2**). Ventricular activation times measured between the RV apex and the LV epicardial free wall were not different in Cx45OE compared to WT hearts (**Table S3**). Activation times obtained from these mice (C57BL6) were comparable to those obtained in mice in the FVB background (**Table S1**).

Because overall conduction velocities were not different in Cx45OEs, we quantified the spatial inhomogeneity in conduction by calculating an inhomogeneity index in a group of eight hearts (five wild-types and three Cx45OEs) from optical action potential data, as reported by Lammers et al.[44] We paced each heart from the right atrium (n = 7) or high right septum (in one WT heart) at a basic cycle length of 180 ms. Activation times were obtained from optical action potentials collected from the LV lateral free wall. A small but significant increase in the inhomogeneity index of Cx45OE hearts was not accompanied by a difference in the absolute inhomogeneity of ventricular conduction in Cx45OE hearts (**Table S4**). Additional S1 or S1/S2 pacing protocols applied to the ventricles did not result in any significant differences in inhomogeneity indices between Cx45OE and WT hearts (data not shown). Thus, neither 85% reduction nor 2-fold overexpression of Cx45 significantly altered electrophysiological properties of the intact heart in vitro.

High-resolution identification of Ser phosphorylation sites on the Cx45 CT tail. The mechanism(s) responsible for controlling Cx45 protein expression levels are not known. Phosphorylation and/or dephosphorylation of Cx43 have/has been implicated in turnover of Cx43 after myocardial ischemic

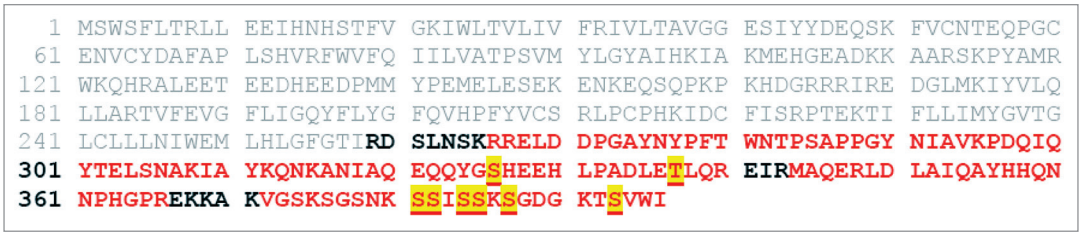

Figure 6. Sequence of mouse Cx45 (NCBI: X63100). Amino acid residues in black and red bold font indicate the sequence of the C-terminus included in the six His-Cx45 CT fusion protein analyzed by mass spectrometry. We obtained 89% coverage of this sequence (red). Seven Ser and one Thr residues (highlighted, red underscored) were phosphorylated by CaMKII in vitro as identified by tandem mass spectrometry. Spectra and tables of fragmentation ions are given in the **Supplemental Content**.

injury. Cx45 is known to be a phosphoprotein;[47-49] however, it has not been studied as extensively as Cx43 with respect to phosphorylation at specific residues in the CT tail or with regard to specific protein kinases that may phosphorylate Cx45. In the present study, we subjected the six His-Cx45 CT fusion protein to phosphorylation by CaMKII and identified seven Ser (S326, S381, S382, S384, S385, S387, S393) and one Thr (T337) residues by high resolution mass spectrometry with 89% coverage of the Cx45 CT sequence (**Fig. 6**) that were targets of CaMKII in vitro. No phospho-peptides were identified in the negative control samples. Extracted ion chromatograms, MS1 and MS2 spectra (**Figs. S6–S10**) and tables of theoretical and observed peptide fragmentation ions (**Tables S5–S9**) are included in the **Supplemental Content** for each phospho-peptide identified. Interestingly, five of the seven Ser residues that were phosphorylated by CaMKII were also found to be phosphorylated in vitro by CK1 (S326, S382, S384, S387, S393) as shown in **Figures S11–S14 and Tables S10–S13**.

Discussion

Residual Cx45 protein levels and heteromeric gap junctions in ventricular myocardium. Several studies have demonstrated that Cx45 is expressed in working ventricular myocardium and isolated myocytes.[13,16-19] Although its protein level in normal, disease-free hearts is very low, the absolute amount of its protein expression had not been established. Furthermore, ultrastructural and biochemical evidence of Cx43/Cx45 heteromeric gap junctions in native ventricular myocardium was lacking. In the present study, we have obtained evidence from immunogold electron microscopy as well as co-immunoprecipitation studies that supports the co-existence of Cx43 and Cx45 in native murine ventricular gap junctions. We used these two complementary approaches to demonstrate presence of both Cx43 and Cx45 in cardiac gap junctions. Immunogold labeling identified both Cx43 and Cx45 in individual gap junctions in intact sections in which cell and tissue architecture were preserved. Immunolabeling of membrane fractions enriched in gap junctions allowed us to quantify the relative abundance of Cx43 and Cx45 in these preparations, and biochemical studies confirmed co-immunoprecipitation of Cx43 and Cx45. In addition, based on quantitative immunoblotting, we report that the magnitude of Cx43 expression in native ventricular myocardium is ~200 fmol/μg protein, and that Cx43 is ~300 times more abundant than Cx45 (**Table 1**). Similar expression levels of integral membrane proteins have been reported based on quantitative immunoblot analyses. McDonald et al.[50] reported 70–80 fmol Na^+-Ca^{2+} exchanger/μg protein in left and right ventricles of guinea pig hearts. Valiunas et al.[51] found 100–500 fmol Cx40 and Cx43/μg protein in HeLa cell transfectants. Recently, Lin et al.[52] reported 400 fmol Cx43/μg protein in ventricular tissue homogenates from neonatal mice.

Changes in Cx45 protein levels do not adversely affect cardiac electrophysiological properties. The absence of measurable abnormal electrophysiological properties in cardiac Cx45-deficient and Cx45OE hearts is consistent with low levels of expression of Cx45 in tissue that has a large reserve of Cx43.[53-56] It should be noted, however, that lack of a measurable defect does not prove absence of a defect in Cx45 transgenic mice. These studies do not address whether altered levels of Cx45 contribute to electrophysiological abnormalities in diseased hearts or in those in which acute or chronic remodeling of Cx43 may have occurred due to aging, injury or other metabolic changes. In addition, closer examination of regions of the heart known to express Cx45 may reveal subtle functional differences when Cx45 is downregulated. For example, there are regions of the AV node in which Cx43 is significantly reduced or absent.[57,58] Presumably, impulses propagate through Cx45 gap junction channels in this part of the AV junction and could be altered if expression of Cx45 is reduced. Similarly, regions of the SA node have been reported to express Cx45 alone (no Cx40 or Cx43),[46] but both Cx30.2 and Cx30 are expressed in the SA node[6,12] and may explain why we saw no sinus alterations in Cx45floxed mice. Finally, one area of interest that deserves greater scrutiny is the Purkinje system and Purkinje-myocyte junction. Recently, several elegant studies have highlighted the importance of the distal conduction system in triggering ventricular arrhythmias.[59] Our studies did not allow us to quantify properties of the distal conduction system at high enough resolution to rule out any defects in Purkinje fibers or their coupling with ventricular myocytes in Cx45-deficient hearts.

Post-translational modification of Cx45 by CaMKII. Our data demonstrating the existence of heteromeric gap junction channels in native ventricular myocardium combined with the observation that the ratio of Cx43:Cx45 not only regulates gap junctional intercellular communication,[23-25,34-36] but gap junction size itself,[17,60] suggest that the number and size of gap junctions in Cx45 transgenic hearts may be altered. The mechanisms underlying

connexin remodeling in heteromeric gap junctions in health and disease are incompletely understood. Post-translational modification, specifically phosphorylation, is known to regulate connexin function and turnover. Phosphorylation of Cx45 has been shown to stabilize Cx45,[49] and to increase or decrease junctional conductance.[61] However, little is known about the signaling pathways that may be involved in phosphorylation of Cx45. Our data (**Fig. 6 and Figs. S6–S10 and Tables S5–S9**) are the first to identify, by mass spectrometry, residues phosphorylated by the multifunctional protein kinase, CaMKII. Importantly, activation of CaMKII has been shown to play a role in development of cardiac hypertrophy, heart failure, myocardial ischemia and infarction.[62-66] Several of the residues phosphorylated by CaMKII were also phosphorylated by CK1 (**Figs. S11–S14 and Tables S10–S13**). Future studies will be required to determine whether CaMKII or CK1 phosphorylates Cx45 in vivo and whether this phosphorylation is altered in cardiac disease states to an extent that can influence cell-to-cell electrical coupling and propagation of action potentials.

Limitations of the study. Although our data indicate that Cx45 and Cx43 coexist in native ventricular gap junctions in the relative proportions reported, our data do not allow us to distinguish between heteromeric and heterotypic channels. Based on the large sizes of the gap junctions identified and quantified in the present study, we suggest that they likely originated from myocytes; however, we cannot rule out the possibility that at least a fraction of the observed Cx45 signal may be attributed to other cell types. Nor have we assessed the relative contribution of Cx45 and Cx43 to gap junction intercellular communication in ventricular myocytes. Furthermore, we have not yet determined the physiological relevance of phosphorylation of Cx45 at the specific residues reported in this study, and whether phosphorylation may regulate assembly or function of heteromeric gap junction channels in vivo. Our data show that global measures of activation and conduction are not altered in Cx45OE hearts; thus, we have yet to establish a mechanism for increased arrhythmia susceptibility in Cx45OEs. The role of Cx45 in the proximal or distal conduction system has not been investigated in sufficient detail to know whether alterations in the expression level of Cx45 alone, or superimposed on a background of remodeled Cx43 in diseased hearts, may be pathophysiologically relevant in mice or in man. Finally, although it appears that an 85% reduction in Cx45 in $Cre^{+};Cx45^{fl/fl}$ mice has modest effects on viability and cardiac function, the Cre-lox transgenic mouse produced in the present study did not result in total ablation of Cx45 (**Figs. 4 and 5**). There are two major hypotheses that may explain the selection of surviving $Cre^{+};Cx45^{fl/fl}$ mice. First, expression of the α-MHC promoter may be delayed (even by only one to a few hours) in those mice that survive, such that deletion of Cx45 may be delayed until after the time when its expression is essential for development and viability. Survival of viable lines from individual founders suggests that delayed expression of the α-MHC promoter may be heritable (perhaps due to epigenetic effects), and thus persists in subsequent generations. Alternatively, survival of $Cre^{+};Cx45^{fl/fl}$ mice may reflect only partial ablation of Cx45, whereby either a threshold level of Cx45 or a certain number of Cx45-expressing cells is sufficient for survival.

Materials and Methods

Animals were handled in accordance with the *NIH Guide for the Care and Use of Laboratory Animals*. The Washington University Animal Studies Committee approved all protocols used in the present study.

Cx45 transgenic mice. *Cx45 overexpressing mice.* Wild-type (WT) and transgenic mice (C57BL6 strain) with cardiac-selective overexpression of Cx45 (Cx45OEs) were maintained in a standard barrier facility. Genotyping and characterization of these mice have been reported previously in reference 20.

Cx45 knockout mice. Embryos with genetic ablation of Cx45 were obtained after timed matings (10.5 days after visualization of a vaginal plug) of $Cx45^{+/-}$ mice.[13] Uteruses were removed from anesthetized mice. The yolk sac was used for PCR genotyping of each individual embryo according to previously published protocols.[37] Embryos were homogenized separately for individual immunoblot analysis.

Cardiac Cx45-deficient mice. Cx45 floxed mice[37] were bred with α-myosin heavy chain (MHC)-Cre^{+} mice[38] to create cardiac-restricted ablation of Cx45. Two polymerase chain reactions (PCR) were run for each sample of DNA using the following primers to assess for presence of Cx45 floxed alleles:

I3Frev 5'-CTC TAG GAA CAC TGT AAC CTG AGA TGT CCC-3'

I5FCfor 5'-GGA TTA AAG GCA TGT GTC ACC ACT CTT GGC-3'

IE3rev 5'-AAG AAC GGC CAC AAC TCT GGT AAC AGG AAG-3'

and the following primers to assess for presence of the Cre recombinase gene:

MHC-Cre, forward 5'-ATG ACA GAC AGA TCC CTC CTA TCT CC-3'

MHC-Cre, reverse 5'-CTC ATC ACT CGT TGC ATC GAC-3'

Results from mice (FVB strain) of the following three genotypes were pooled and used as controls for the cardiac Cx45-deficient ($Cre^{+};Cx45^{fl/fl}$) mice: $Cre^{-};Cx45^{+/+}$, $Cre^{+};Cx45^{fl/+}$, $Cre^{-};Cx45^{fl/fl}$.

Cx40 knockin Cx45 atria. Atrial tissue samples from Cx40 knockin Cx45 mice ($Cx40^{KICx45/KICx45}$) [39] were obtained from Dr. Patrick Jay with the generous permission of Dr. Daniel Gros. These atrial samples which lack expression of Cx40 and exhibit expression of Cx45 (knocked into the Cx40 locus) served as negative controls for Cx40 expression and positive controls for Cx45 expression.

Gap junction-enriched membrane preparations. Gap junction-enriched membrane fractions were prepared using a procedure published by Kensler and Goodenough[40] using sucrose density centrifugation as described in detail in the **Supplemental Content**. The final yield of the gap junction-enriched fraction was 3–9 μg protein per g of heart (wet weight).

Quantitative immunoblot analysis. Six His-Cx45 carboxyl-terminal (CT) and glutathione S-transferase (GST)-Cx43 CT fusion protein constructs were grown and purified as described in detail in the **Supplemental Content**. Ventricular homogenates, six His-Cx45 CT fusion protein and GST-Cx43 CT fusion

protein were each run in different lanes. Three separate Cx45 CT and three separate Cx43 CT fusion protein preparations were used in the quantitative immunoblots reported here (**Fig. S1**).

Ventricular homogenates from a total of 16 hearts were run on nine separate gels as described in the **Supplemental Content** for quantitative immunoblot analysis. Standard fusion protein curves were calculated in Excel and the ng of connexin protein per 15 μg protein loaded in each lane were converted to fmol/μg of total protein.

Immunoprecipitations. We performed co-immunoprecipitation experiments on murine ventricles that were flash frozen, pulverized, homogenized and lysed as described in detail in the **Supplemental Content** using monoclonal anti-Cx45 or anti-Cx43 antibody bound to protein G sepharose. A nonspecific IgG1 was used as a negative control.

Immunogold electron microscopy. Ventricular tissue samples, cut with a vibratome, and isolated gap junction-enriched membrane preparations were stained using a pre-embedding procedure published previously in references 41 and 42 as described in the **Supplemental Content**.

Immunostaining and confocal analysis. Ten-μm frozen sections were incubated in rabbit anti-Cx45, rabbit anti-Cx43 or goat anti-Cx40 antibodies and analyzed on a Zeiss LSM-510 META confocal microscope as described in detail in the **Supplemental Content**. A total of five Cre^{+};$Cx45^{fl/fl}$ and eight control hearts were stained in four experiments. Adjacent tissue sections were stained with anti-Cx45, anti-Cx43, anti-Cx40 and secondary (alone) antibodies for each experiment. Confocal images for a given antibody and experiment were acquired on the same day with identical confocal microscope settings. An investigator blinded to genotype quantified immunoreactive signal using ImageJ software. Gap junction staining was defined as five or more contiguous pixels.

Anti-Cx45 polyclonal antibody production. The same six His-Cx45 CT fusion protein used in the quantitative immunoblots was used as antigen to immunize rabbits for production of anti-Cx45 antiserum at Pocono Rabbit Farm & Laboratory; antiserum was affinity purified and characterized as described in detail in the **Supplemental Content** (**Fig. S2**).

In vitro electrophysiology studies of cardiac Cx45 transgenic mice. C57BL6 WT (n = 6) and Cx45OEs (n = 4) were anesthetized with Avertin (0.1 mg/kg) followed by removal and retrograde perfusion of hearts via the aorta at 25°C[43] for in vitro electrophysiology studies and optical mapping as described in detail in the **Supplemental Content**. Inhomogeneity indices were calculated as described by Lammers et al.[44] and in the **Supplemental Content**.

A total of 11 FVB controls and four cardiac Cx45-deficient Cre^{+};$Cx45^{fl/fl}$ mice were subjected to limited electrophysiological testing in vitro as described in the **Supplemental Content**. Surface ECGs were recorded from nine mice (n = 5 controls and n = 4 Cx45-deficient). Optical maps were obtained from five mice (n = 3 controls and n = 2 Cx45-deficient). Activation times were measured in 10 mice (n = 8 controls and n = 2 Cx45-deficient).

High-resolution mass spectrometric identification of Cx45 phosphorylation sites. Cx45 CT fusion protein was subjected to in vitro phosphorylation using either Ca^{2+}/calmodulin-dependent kinase II (CaMKII, New England Biolabs) or casein kinase 1 (CK1, New England Biolabs) per the manufacturer's instructions, and subjected to tandem mass spectrometry using a Thermo LTQ XL Orbitrap (Thermo Fisher, San Jose, CA) as described previously in reference 45.

Statistical analysis. All values are expressed as mean ± SD .Two group comparisons were made using Student's t-test for grouped data. A value of $p < 0.05$ was considered significant.

Conclusions

The data presented here using a newly derived, fully characterized polyclonal anti-Cx45 antibody corroborates previous reports of expression of the minor ventricular connexin, Cx45, by working ventricular myocytes.[13,16-19,30-33] We have determined that the levels of Cx45 are 0.3% of those of Cx43, and that cardiac-restricted genetic downregulation or overexpression of Cx45 does not result in any notable deficits in electrical conduction throughout the heart under disease-free conditions. It is possible that downregulation of Cx43 with concomitant upregulation of Cx45 could shift the relative stoichiometry of these two connexins within heteromeric gap junctions in remodeled ischemic or failing hearts. Finally, the role of CaMKII in regulating cardiac Cx45 under both normal and pathophysiologic conditions merits further investigation.

Disclosure of Potential Conflicts of Interest

No potential conflicts of interest were disclosed.

Acknowledgments

The authors would like to thank Dr. Thomas H. Steinberg for the generous gifts of Cx45 fusion protein construct, anti-Cx45 antiserum and connexin-expressing HeLa cells; Dr. Patrick Y. Jay for assistance and guidance with embryo dissection, sectioning of the conduction system and $Cx40^{KICx45}$ tissue procurement; Dr. Michael Schneider for use of his α-MHC-Cre mice; Dr. Daniel Gros for the generous gift of $Cx40^{KICx45}$ atria; Dr. Chaobin Hu and Erin M. Gribben for expert technical help; William J. Kraft and Karen G. Green in the Department of Pathology and Immunology Research Electron Microscopy Core for performing the immunogold double labeling experiments; William Coleman and Marlene Scott in the Histology and Microscopy Core for cutting all of the tissue sections; Petra Gilmore in the Proteomics Core for expert sample preparation; and the Mouse Genetics Core for mouse husbandry support. Mice were housed in a facility supported by NIH National Centers for Research Resources (NCRR) Grant C06 RR015502. This work was supported by NIH NCRR Grant 2P41RR000954 and UL1 RR024992, a grant (Wi270/29-1) from the German Research Foundation (Klaus Willecke), and NIH/NHLBI Grant HL-066350 (Kathryn A. Yamada).

Note

Supplemental material can be found at:
http://www.landesbioscience.com/admin/article/18523/

References

1. Veenstra RD, Wang HZ, Beyer EC, Brink PR. Selective dye and ionic permeability of gap junction channels formed by connexin45. Circ Res 1994; 75:483-90.
2. Moreno AP, Saez JC, Fishman GI, Spray DC. Human connexin43 gap junction channels. Regulation of unitary conductances by phosphorylation. Circ Res 1994; 74:1050-7.
3. Beblo DA, Wang HZ, Beyer EC, Westphale EM, Veestra RD. Unique conductance, gating and selective permeability properties of gap junction channels formed by connexin40. Circ Res 1995; 77:813-22.
4. Bukauskas FF, Elfgang C, Willecke K, Weingart R. Biophysical properties of gap junction channels formed by mouse connexin40 in induced pairs of transfected human HeLa cells. Biophys J 1995; 68:2289-98.
5. Kanno S, Saffitz JE. The role of myocardial gap junctions in electrical conduction and arrhythmogenesis. Cardiovasc Pathol 2001; 10:169-77.
6. Coppen SR, Severs NJ, Gourdie RG. Connexin 45 (α6) expression delineates an extended conduction system in the embryonic and mature rodent heart. Dev Genet 1999; 24:82-90.
7. Bukauskas FF, Kreuzberg MM, Rackauskas M, Bukauskiene A, Bennett MVL, Verselis VK, et al. Properties of mouse connexin 30.2 and human connexin 31.9 hemichannels: implications for atrioventricular conduction in the heart. Proc Natl Acad Sci 2006; 103:9726-31.
8. Kreuzberg MM, Liebermann M, Segschneider S, Dobrowolski R, Dobrzynski H, Kaba R, et al. Human connexin31.9, unlike its orthologous protein connexin30.2 in the mouse, is not detectable in the human cardiac conduction system. J Mol Cell Cardiol 2009; 46:553-9.
9. Bastide B, Neyses L, Ganten D, Paul M, Willecke K, Traub O. Gap junction protein connexin40 is preferentially expressed in vascular endothelium and conductive bundles of rat myocardium and is increased under hypertensive conditions. Circ Res 1993; 73:1138-49.
10. Gourdie RG, Severs NH, Green CR, Rothery S, Germroth P, Thompson RP. The spatial distribution and relative abundance of gap-junctional connexin40 and connexin43 correlate to functional properties of components of the cardiac atrioventricular conduction system. J Cell Sci 1993; 105:985-91.
11. Saffitz JE, Kanter HL, Green KG, Tolley TK, Beyer EC. Tissue-specific determinants of anisotropic conduction velocity in canine atrial and ventricular myocardium. Circ Res 1994; 74:1065-70.
12. Gros D, Théveniau-Ruissy M, Bernard M, Calmels T, Kober F, Söhl G, et al. Connexin 30 is expressed in the mouse sino-atrial node and modulates heart rate. Cardiovasc Res 2010; 85:45-55.
13. Krüger O, Plum A, Kim JS, Winterhager E, Maxeiner S, Hallas G, et al. Defective vascular development in connexin 45-deficient mice. Development 2000; 127:4179-93.
14. Kumai M, Nishii K, Nakamura K, Takeda N, Suzuki M, Shibata Y. Loss of connexin45 causes a cushion defect in early cardiogenesis. Development 2000; 127:3501-12.
15. Coppen SR, Dupont E, Rothery S, Severs NJ. Connexin45 expression is preferentially associated with the ventricular conduction system in mouse and rat heart. Circ Res 1998; 82:232-43.
16. von Maltzahn J, Kreuzberg MM, Matern G, Euwens C, Höher T, Wörsdörfer P, et al. C-terminal tagging with eGFP yields new insights into expression of connexin45 but prevents rescue of embryonic lethal connexin45-deficient mice. Eur J Cell Biol 2009; 88:481-94.
17. Johnson CM, Green KG, Kanter EM, Bou-Abboud E, Saffitz JE, Yamada KA. Voltage-gated Na^+ channel activity and connexin expression in Cx43-deficient myocytes. J Cardiovasc Electrophysiol 1999; 10:1390-401.
18. Yamada KA, Rogers JG, Sundset R, Steinberg TH, Saffitz JE. Upregulation of connexin45 in heart failure. J Cardiovasc Electrophysiol 2003; 14:1205-12.
19. Beauchamp P, Choby C, Desplantez T, de Peyer K, Green K, Yamada KA, et al. Electrical propagation in synthetic ventricular myocyte strands from germline connexin43 knock out mice. Circ Res 2004; 95:170-8.
20. Betsuyaku T, Nnebe NS, Sundset R, Patibandla S, Krueger CM, Yamada KA. Overexpression of cardiac connexin45 increases susceptibility to ventricular tachyarrhythmias in vivo. Am J Physiol Heart Circ Physiol 2006; 290:H163-71.
21. White TW, Paul DL, Goodenough DA, Bruzzone R. Functional analysis of selective interactions among rodent connexins. Mol Biol Cell 1995; 6:459-70.
22. Elfgang C, Eckert R, Lichtenberg-Frate H, Butterweck A, Traub O, Klein RA, et al. Specific permeability and selective formation of gap junction channels in connexin-transfected HeLa cells. J Cell Biol 1995; 129:805-17.
23. Moreno AP, Fishman GI, Beyer EC, Spray DC. Voltage dependent gating and single channel analysis of heterotypic channels formed by Cx45 and Cx43. Prog Cell Res 1995; 4:405-8.
24. Koval M, Geist ST, Westphale EM, Kemendy EM, Civitelli R, Beyer EC, et al. Transfected connexin45 alters gap junction permeability in cells expressing endogenous connexin43. J Cell Biol 1995; 130:987-95.
25. Steiner E, Ebihara L. Functional characterization of canine connexin45. J Membr Biol 1996; 150:153-61.
26. He DS, Burt JM. Function of gap junction channels formed in cells co-expressing connexin40 and 43. In: Werner R, Ed. Gap Junctions. Amsterdam: IOS Press 1998; 40-4.
27. Valiunas V, Weingart R, Brink PR. Formation of heterotypic gap junction channels by connexins 40 and 43. Circ Res 2000; 86:e42-9.
28. Moreno AP. Biophysical properties of homomeric and heteromultimeric channels formed by cardiac connexins. Cardiovasc Res 2004; 62:276-86.
29. Rackauskas M, Kreuzberg MM, Pranevicius M, Willecke K, Verselis VK, Bukauskas FF. Gating properties of heterotypic gap junction channels formed of connexins 40, 43 and 45. Biophys J 2007; 92:1952-65.
30. Chen YH, DeHaan RL. Multiple-channel conductance states and voltage regulation of embryonic chick cardiac gap junctions. J Membr Biol 1992; 127:95-111.
31. Verheule S, van Kempen MJA, te Welscher PHJA, Kwak BR, Jongsma HJ. Characterization of gap junction channels in adult rabbit atrial and ventricular myocardium. Circ Res 1997; 80:673-81.
32. Valiunas V, Bukauskas FF, Weingart R. Conductances and selective permeability of connexin43 gap junction channels examined in neonatal rat heart cells. Circ Res 1997; 80:708-19.
33. Elenes S, Rubart M, Moreno AP. Junctional communication between isolated pairs of canine atrial cells is mediated by homogeneous and heterogeneous gap junction channels. J Cardiovasc Electrophysiol 1999; 10:990-1004.
34. Martinez AD, Hayrapetyan V, Moreno AP, Beyer EC. Connexin43 and connexin45 form heteromeric gap junction channels in which individual components determine permeability and regulation. Circ Res 2002; 90:1100-7.
35. Elenes S, Martinez AD, Delmar M, Beyer EC, Moreno AP. Heterotypic docking of Cx43 and Cx45 connexons blocks fast voltage gating of Cx43. Biophys J 2001; 81:1406-18.
36. Bukauskas FF, Bukauskiene A, Verselis VK, Bennett MVL. Coupling asymmetry of heterotypic connexin 45/connexin 43-EGFP gap junctions: properties of fast and slow gating mechanisms. Proc Natl Acad Sci USA 2002; 99:7113-8.
37. Maxeiner S, Dedek K, Janssen-Bienhold U, Ammermüller J, Brune H, Kirsch T, et al. Deletion of connexin45 in mouse retinal neurons disrupts the rod/cone signaling pathway between AII amacrine and ON cone bipolar cells and leads to impaired visual transmission. J Neurosci 2005; 25:566-76.
38. Agah R, Frenkel PA, French BA, Michael LH, Overbeek PA, Schneider MD. Gene recombination in postmitotic cells: targeted expression of Cre recombinase provokes cardiac-restricted, site-specific rearrangement in adult ventricular muscle in vivo. J Clin Invest 1997; 100:169-79.
39. Alcoléa S, Jarry-Guichard T, de Bakker J, Gonzàlez D, Lamers W, Coppen S, et al. Replacement of connexin40 by connexin45 in the mouse: impact on cardiac electrical conduction. Circ Res 2004; 94:100-9.
40. Kensler RW, Goodenough DA. Isolation of mouse myocardial gap junctions. J Cell Biol 1980; 86:755-64.
41. Kanter HL, Laing JG, Beyer EC, Green KG, Saffitz JE. Multiple connexins colocalize in canine ventricular myocyte gap junctions. Circ Res 1993; 73:344-50.
42. Luke RA, Beyer EC, Hoyt RH, Saffitz JE. Quantitative analysis of intercellular connections by immunohistochemistry of the cardiac gap junction protein connexin43. Circ Res 1989; 65:1450-7.
43. Lerner DL, Yamada KA, Schuessler RB, Saffitz JE. Accelerated onset and increased incidence of ventricular arrhythmias induced by ischemia in Cx43-deficient mice. Circulation 2000; 101:547-52.
44. Lammers WJEP, Schalij MJ, Kirchhof CJHJ, Allessie MA. Quantification of spatial inhomogeneity in conduction and initiation of reentrant atrial arrhythmias. Am J Physiol Heart Circ Physiol 1990; 259:H1254-63.
45. Huang RYC, Laing JG, Kanter EM, Berthoud VM, Bao M, Rohrs HW, et al. Identification of CaMKII phosphorylation sites in connexin43 by high-resolution mass spectrometry. J Proteome Res 2011; 10:1098-109.
46. Verheijck EE, van Kempen MJA, Veereschild M, Lurvink J, Jongsma HJ, Bouman LN. Electrophysiological features of the mouse sinoatrial node in relation to connexin distribution. Cardiovasc Res 2001; 52:40-50.
47. Laing JG, Westphale EM, Engelmann GL, Beyer EC. Characterization of the gap junction protein, connexin45. J Membr Biol 1994; 139:31-40.
48. Butterweck A, Gergs U, Elfgang C, Willecke K, Traub O. Immunochemical characterization of the gap junction protein connexin45 in mouse kidney and transfected human HeLa cells. J Membr Biol 1994; 141:247-56.
49. Hertlein B, Butterweck A, Haubrich S, Willecke K, Traub O. Phosphorylated carboxy terminal serine residues stabilize the mouse gap junction protein connexin45 against degradation. J Membr Biol 1998; 162:247-57.
50. McDonald RL, Colyer J, Harrison SM. Quantitative analysis of Na^+-Ca^{2+} exchanger expression in guinea-pig heart. Eur J Biochem 2000; 267:5142-8.
51. Valiunas V, Gemel J, Brink PR, Beyer EC. Gap junction channels formed by coexpressed connexin40 and connexin43. Am J Physiol Heart Circ Physiol 2001; 281:H1675-89.
52. Lin X, Gemel J, Glass A, Zemlin CW, Beyer EC, Veenstra RD. Connexin40 and connexin43 determine gating properties of atrial gap junction channels. J Mol Cell Cardiol 2010; 48:238-45.
53. Jongsma HJ, Wilders R. Gap junctions in cardiovascular disease. Circ Res 2000; 86:1193-7.
54. Gutstein DE, Morley GE, Tamaddon H, Vaidya D, Schneider MD, Chen J, et al. Conduction slowing and sudden arrhythmic death in mice with cardiac-restricted inactivation of connexin43. Circ Res 2001; 88:333-9.
55. Eckardt D, Theis M, Degen J, Ott T, van Rijen HVM, Kirchhoff S, et al. Functional role of connexin43 gap junction channels in adult mouse heart assessed by inducible gene deletion. J Mol Cell Cardiol 2004; 36:101-10.

56. van Rijen HVM, de Bakker JMT, van Veen TAB. Hypoxia, electrical uncoupling and conduction slowing: role of conduction reserve. Cardiovasc Res 2005; 66:9-11.
57. Li J, Greener ID, Inada S, Nikolski VP, Yamamoto M, Hancox JC, et al. Computer three-dimensional reconstruction of the atrioventricular node. Circ Res 2008; 102:975-85.
58. Hucker WJ, McCain ML, Laughner JI, Iaizzo PA, Efimov IR. Connexin 43 expression delineates two discrete pathways in the human atrioventricular junction. Anat Rec 2008; 291:204-15.
59. Cerrone M, Noujaim SF, Tolkacheva EG, Talkachou A, O'Connell R, Berenfeld O, et al. Arrhythmogenic mechanisms in a mouse model of catecholaminergic polymorphic ventricular tachycardia. Circ Res 2007; 101:1039-48.
60. Grikscheit K, Thomas N, Bruce AF, Rothery S, Chan J, Severs NJ, et al. Coexpression of connexin45 with connexin43 decreases gap junction size. Cell Commun Adhes 2008; 15:185-93.
61. van Veen TAB, van Rijen HVM, Jongsma HJ. Electrical conductance of mouse connexin45 gap junction channels is modulated by phosphorylation. Cardiovasc Res 2000; 46:496-510.
62. Hagemann D, Bohlender J, Hoch B, Krause EG, Karczewski P. Expression of Ca^{2+}/calmodulin-dependent protein kinase II δ-subunit isoforms in rats with hypertensive cardiac hypertrophy. Mol Cell Biochem 2001; 220:69-76.
63. Backs J, Backs T, Neef S, Kreusser MM, Lehmann LH, Patrick DM, et al. The δ isoform of CaM kinase II is required for pathological cardiac hypertrophy and remodeling after pressure overload. Proc Natl Acad Sci 2009; 106:2342-7.
64. Hoch B, Meyer R, Hetzer R, Krause EG, Karczewski P. Identification and expression of δ-isoforms of the multifunctional Ca^{2+}/calmodulin-dependent protein kinase in failing and nonfailing human myocardium. Circ Res 1999; 84:713-21.
65. Vila-Petroff M, Salas MA, Said M, Valverde CA, Sapia L, Portiansky E, et al. CaMKII inhibition protects against necrosis and apoptosis in irreversible ischemia-reperfusion injury. Cardiovasc Res 2007; 73:689-98.
66. Yoo B, Lemaire A, Mangmool S, Wolf MJ, Curcio A, Mao L, et al. β1-Adrenergic receptors stimulate cardiac contractility and CaMKII activation in vivo and enhance cardiac dysfunction following myocardial infarction. Am J Physiol Heart Circ Physiol 2009; 297:H1377-86.